Development of a Novel Binder Using Lime and Incinerated Sewage Sludge Ash to Stabilize and Solidify Contaminated Marine Sediments with High Water Content as a Fill Material

Jiang-shan Li, Ph.D.[1]; Yi-fan Zhou, Ph.D.[2]; Qi-ming Wang, Ph.D.[3]; Qiang Xue, Ph.D.[4]; and Chi Sun Poon, Ph.D.[5]

Abstract: In this study, incinerated sewage sludge ash (ISSA) was applied to replace ordinary portland cement (OPC) and quick (unhydrated) lime at different ratios of 0%, 20%, and 50% for improving the properties of marine sediments with high water content by solidification/stabilization (S/S) method. Then, the effects of different binders and curing time (7 and 28 days) on sediment properties, including unconfined compressive strength (UCS), shear strength, durability, and leachability of metals were investigated. Test results indicated that lime–ISSA binder had several advantages over OPC–ISSA binder owing to its lower cost, lower environmental footprints, and better strength gains. The UCS, deformation resistance, and shear strength of the specimens prepared using lime as the binder were improved with the increasing addition of ISSA, and the water permeability was also effectively reduced. The results of environmental impact assessment (in particular leaching characteristics) indicated that the leachability of heavy metals in the lime–ISSA stabilized sediments was effectively mitigated. The proposed fill material complied with the acceptance criteria for engineering fills applications. A series of spectroscopic/microscopic laboratory tests including mercury intrusion porosimetry (MIP), thermogravimetric analysis (TGA), scanning electron microscopy (SEM), and X-ray diffraction (XRD) were performed to investigate the mechanisms controlling strength development and metals immobilization. The chemical reactions between the sediments, ISSA, and lime resulted in the formation of hydrated cementitious compounds that facilitated the decrease in pore volume and increase in strength and stabilization of heavy metals. On the whole, the lime–ISSA system could replace the OPC–ISSA binder to particularly improve the geotechnical and environmental properties of the contaminated sediments. **DOI: 10.1061/(ASCE)MT.1943-5533.0002913.**

Author keywords: Contaminated marine sediment; Incinerated sewage sludge ash; Solidification/stabilization; Heavy metals; Fill material.

Introduction

To maintain sufficient depth in harbors for navigation and clean seawater, marine sediments are dredged routinely throughout the world (Couvidat et al. 2018; Libralato et al. 2018). These sediments are generally contaminated with inorganic components (heavy metals, metalloid elements and some salts such as sulfate, chloride, and nitrate) and organic components (polycyclic aromatic hydrocarbons, polychlorobiphenyl, and organochlorine pesticides) due to various human activities, which presents a serious threat to the environment if dredged and disposed without any treatment (Saussaye et al. 2016; Falciglia et al. 2018). In Hong Kong, approximately 29 Mm^3 of dredged sediments were classified as unacceptably contaminated and were required to be disposed (Wang et al. 2015). The traditional methods for the disposal of the contaminated sediments, such as land deposit and ocean immersion, are gradually being abandoned by more and more countries because suitable disposal locations are running out and because of more stringent environmental regulations (Wang et al. 2013b).

In order to ensure the sustainable management of contaminated sediment, solidification/stabilization (S/S) processes and/or valorization of the contaminated sediments as secondary raw materials in civil engineering are promoted, which can improve the physical, mechanical, and environmental properties of the dredged sediments via chemical and physical means (Lofrano et al. 2017). Additionally, they not only fulfil the safe treatment, but also provide resource recycling approaches of contaminated sediments. Many published studies have shown that the S/S treated sediments were suitable to be used as civil engineering fills and road subbases, for cement and concrete production, and for brick fabrication (Dang et al. 2013; Achour et al. 2014; Wang et al. 2017b). Previous studies have successfully recycled contaminated sediment as useful

[1]Postdoctoral Researcher, Dept. of Civil and Environmental Engineering, Hong Kong Polytechnic Univ., Hung Hom, Kowloon, Hong Kong; Associate Professor, State Key Laboratory of Geomechanics and Geotechnical Engineering, Institute of Rock and Soil Mechanics, Chinese Academy of Sciences, Wuhan 430071, China. ORCID: https://orcid.org/0000-0003-0055-7397. Email: jiangshan.li@polyu.edu.hk; jsli@whrsm.ac.cn

[2]Master, Dept. of Civil and Environmental Engineering, Hong Kong Polytechnic Univ., Hung Hom, Kowloon, Hong Kong. Email: Christina.yf.zhou@connect.polyu.hk

[3]Master, Dept. of Civil and Environmental Engineering, Hong Kong Polytechnic Univ., Hung Hom, Kowloon, Hong Kong. Email: q.m.wang@polyu.edu.hk

[4]Professor, State Key Laboratory of Geomechanics and Geotechnical Engineering, Institute of Rock and Soil Mechanics, Chinese Academy of Sciences, Wuhan 430071, China. Email: qiangx@whrsm.ac.cn

[5]Chair Professor, Dept. of Civil and Environmental Engineering, Hong Kong Polytechnic Univ., Hung Hom, Kowloon, Hong Kong (corresponding author). Email: cecspoon@polyu.edu.hk

Note. This manuscript was submitted on October 18, 2018; approved on May 29, 2019; published online on August 9, 2019. Discussion period open until January 9, 2020; separate discussions must be submitted for individual papers. This paper is part of the ***Journal of Materials in Civil Engineering***, © ASCE, ISSN 0899-1561.

construction materials including fill materials, partition blocks, and paving blocks via the cement-based S/S technology (Wang et al. 2018b, c).

Conventional ordinary portland cement (OPC) is the most prevailing binder used in S/S technology (Chatain et al. 2013). However, its production is very energy intensive and the manufacturing process generates a huge amount of carbon dioxide. Therefore, less energy-intensive, eco-friendly, and economical cementing materials are being sought or explored by researchers and engineers (Wang et al. 2017a; Chen et al. 2018a). A number of supplementary cementitious materials (SCMs) such as pulverized fly ash (PFA) and ground-granulated blast-furnace slag (GGBS) have been used to (partially) replace OPC as alternative binders in the S/S treatment of sediments owing to their lower costs, recycling values, and relatively good pozzolanic activities for strength gain (Zentar et al. 2012; Shim et al. 2016; Wang et al. 2018a). The study by Wang et al. (2018a) found that fly ash improved the strength and modulus of lime-solidified sediments but weakened the mechanical characteristics of cement-solidified sediments. Tang et al. (2015) mixed 75% by mass of contaminated marine mud and sediment, respectively, with 20% and 5% of cement and PFA, and obtained unconfined compressive strengths (UCS) of 8.32 and 4.47 MPa, respectively. The aforementioned research studies focused on the improvement of engineering characteristics of S/S treated sediments by OPC–lime incorporated with SCMs. However, few studies can be found on the environmental and microstructural/spectroscopic properties of S/S treated sediment.

Moreover, another waste type of concern is the ash generated from the incineration of sewage sludge. Considering its lower pozzolanic activity than PFA and GGBS, incinerated sewage sludge ash (ISSA) is not commonly used as a SCM (Chen et al. 2018b). Cyr et al. (2007) found that a blended cement containing ISSA caused reduction in compressive and flexural strength of mortars, but such reduction became less over time. The study by Chen and Lin (2009) indicated that the ISSA–cement system had some potential applications in the field of geotechnical engineering. A previous study has also confirmed that ISSA could be used as functional materials in the S/S treatment of contaminated soil with high concentration of lead (Pb) due to the high absorptivity of ISSA toward heavy metals (Li and Poon 2017). Therefore, it is envisaged that ISSA can be used to stabilize heavy metals contaminated sediments to produce low-quality fill materials. However, in Hong Kong currently, it is a pity that most of the ISSA generated is disposed of at landfills, which inevitably results in environmental burden and wasting of resources.

This paper reports on a preliminary study that aimed to develop a new technique that is capable of treating contaminated sediments by using ISSA with lime–OPC-based binder. The produced construction materials can be used as road bases or engineering fills. First, the effects of ISSA incorporation on the stabilized sediments would be revealed by investigating the changes of engineering and environmental properties. Second, the mechanisms of the strength development and heavy metals immobilization were explored by a series of microstructure and spectroscopy analysis.

Materials and Methods

Contaminated Sediment and Cementitious Binders

The contaminated marine sediment was dredged from a near shore location in Hong Kong. The total heavy metals in the sediment were determined by inductively coupled plasma atomic emission spectrometry (ICP-AES) (SPECTROBLUE) after complete acid digestion, and the concentrations were 74.04 mg kg^{-1} of Cu, 154.72 mg kg^{-1} of Zn, 73.58 mg kg^{-1} of Pb, 37.30 mg kg^{-1} of Cr, 16.22 mg kg^{-1} of Ni, 34.08 mg kg^{-1} of As, and 2.18 mg kg^{-1} of Cd. According to the management guideline in Hong Kong, the sediment was classified as moderately contaminated (Category M) (HK ETWB 2002). X-ray fluorescence (XRF) spectrometry (Rigaku Supermini200) was used to determine the major chemical compositions of the dried sediment. SiO_2 (58.05%) and Al_2O_3 (21.99%) were found to be dominant chemical constitutes.

The dredged sediment was found to have 66.5% moisture content, 24.8 g kg^{-1} salinity (WTW inoLab Cond 720), 4.2% organic matter (loss on ignition at 550°C), specific gravity (water pycnometer method) of 2.49, and pH (1:10 dry sample: DI water) of 8.55. The sediment samples were passed through a 5-mm sieve to remove oversize sand and gravel before using in the experiments. The particle size distribution curves (Fig. S1), determined by a Malvern MS3000 laser diffraction equipment in combination with the sieving analysis method, revealed that the studied marine sediment consisted of 0.34% clay fraction, 16.69% silt fraction, 44.64% sand fraction, and 38.33% gravel fraction. Therefore the plastic limit, liquid limit, and plastic index of the sediment could not be determined due to the low viscidity.

The OPC used was from a local manufacture that was equivalent to ASTM Type I cement. A commercially available quick (unhydrated) lime containing 65% of CaO was obtained from International Laboratory USA. The ISSA was collected from a local sewage sludge incinerator (T · PARK) and its chemical and physical characteristics can be found in a previous paper (Li et al. 2017d).

Sediment-Based Fill Material Production

The mix designs of sediment-based fill materials made by OPC–lime with ISSA are summarized in Table 1. All the samples are denoted as (C/L)X, where C/L indicates OPC–lime and X indicates amount in percentage of C/L that was replaced by ISSA. Note that no additional water was added and the binder content was defined as the ratio of the dry mass of binder to the wet mass of the sediment. The sediment mixtures were designed to a density within a typical range of 1,500 to 1,700 kg/m^3 (Yan et al. 2014). The proportioned sediment-binder mixture was mixed uniformly for about 3 min in a mechanical mixer. Thereafter, the fresh mixtures were tested for flow consistency according to ASTM C1437 (ASTM 2007) immediately. All the S/S sediment mixtures showed good workabilities (Table 1). To prepare the hardened S/S samples, the blended mixtures were cast into cylindrical molds with a modest vibration (to release trapped air in the mixture) and then covered with a plastic film to avoid water evaporation. The samples were then stored in a curing room at 20°C ± 2°C and 95% relative humidity. The hardened sediment samples were removed from the curing room and demolded at Day 7 and Day 28 for the following tests.

Table 1. Mix proportions and physical properties of S/S treated sediment

Symbols	OPC (% weight of sediment)	Lime (% weight of sediment)	ISSA (% weight of sediment)	Fresh density (kg/m^3)	Flow table value (cm)
Raw sediment	0	0	0	1,527	19.64
C0	10	—	—	1,599	15.19
C20	8	—	2	1,564	15.02
C50	5	—	5	1,606	14.98
L0	—	10	—	1,582	14.03
L20	—	8	2	1,551	14.28
L50	—	5	5	1,507	14.65

Engineering Properties, Metal(loid)s Leaching, and Microstructure/Microscopic Analyses

Engineering Properties

A loading equipment setup (Testometric CXM 500-50kN) was used to determine the load-displacement curves of the specimens with 50 mm in diameter and 50 mm in height at a loading rate of 0.3 mm/min according to BS EN12390-3 (BSI 2002), which helped to calculate the UCS, failure strain, and deformation modulus. Note that the deformation modulus in this study is defined as the secant modulus at 50% of UCS.

The direct shear tests were performed following BS 1377-7 (BSI 1990b), under four different normal vertical stresses of 50, 100, 200, and 300 kPa, to determine the consolidated-undrained shear strength of the S/S treated sediments. As the test apparatus was originally designed for soil testing and not able to measure shear strength values of over 0.35 MPa, only the samples after 3 days of curing in the cutting ring were tested. The direct shear tests were performed at a shear rate of 0.8 mm/min on the saturated samples with 60 mm in diameter and 20 mm in height. The samples were saturated by applying the vacuum method before being demolded from the cutting ring and transferred into shear box. The direct shear test procedure was implemented for determining the strength parameters Φ (angle of shearing resistance) and C (cohesion intercept) of the material.

The constant head permeability test was performed on a PN3230M flexible-wall permeameter (Geoequip Corporation, Chesapeake, Virginia). The samples tested were with 50 mm in diameter and 50 mm in height according to BS 1377-5 (BSI 1990a), and distilled water was used as the permeation solution. Before testing, all the samples were presaturated in a vacuum saturator for 24 h and filled with distilled water. The confining pressure of the sample was maintained at 100 kPa to prevent side leakages. The water head and room temperature were set at 8 m and 25°C, respectively.

In order to establish the durability of the S/S treated sediment specimens in the wet environment after a curing period of 28 days, the samples were immersed in distilled water for 30 days. Then, the samples were tested to determine the UCS.

Metal(loid)s Leaching

The toxicity characteristic leaching procedure (TCLP) was used to determine the leachability of metal(loid)s in the sediments before and after the S/S treatment [EPA Method 1311 (US EPA 1992)]. The samples were leached with 0.1 M glacial acetic acid (pH 2.88 ± 0.05) at a liquid-to-solid ratio of 20 L kg^{-1} and rotated for 18 h at 30 rpm.

Semidynamic leaching tests were applied to assess the long-term leaching potential of the monolithic samples after the S/S treatment [ASTM C1308 (ASTM 2008)]. The ratio of volume of deionized (DI) water used to the surface area of the specimen was 10:1. The leaching test was conducted for 11 days at a constant temperature of 23°C ± 2°C, in which DI water was renewed after 2, 5, and 17 h in the first day, and then daily for the following 10 days.

Afterward, the solid and the liquid phases of the leachates were separated first by a centrifuge at 4,000 rpm for 10 min and followed by filtration with a 0.45 μm mixed cellulose esters membrane filter. The leachates were subjected to acid digestion by concentrated HNO_3 at a volume ratio of 5:2 (sample:HNO_3) followed by ICP-AES (SPECTROBLUE) analysis. In addition, 2 mg L^{-1} As standard was analyzed every 10 samples for quality control and assurance purposes.

The cumulative fraction leached (CFL) and effective diffusion coefficient of metal(loid)s in the semidynamic leaching tests were calculated according to a previous study (Li et al. 2017c). The previous tests were determined on three samples and the average values were reported. The error bars in the respective figures indicate the standard deviation ($n = 3$).

Spectroscopic/Microscopic Analyses

Spectroscopic/microscopic analyses were conducted on the samples after 28 days of curing. The crystalline-phase mineralogy of the milled samples was evaluated by using a high resolution powdered X-ray diffractometer (XRD) (Rigaku SmartLab, Tokyo, Japan) with a scan degree from 5° to 60° 2θ using CuKα ($\lambda = 1.54059$ Å) radiation obtained at 40 kV and 30 mA.

Thermogravimetric analysis (TGA) (Rigaku Thermo Plus) was performed on the milled samples to study the thermal behavior, and the temperature rose from 30°C to 1,000°C at a heating rate of 5°C min^{-1} under argon gas stripping. A Tescan-Vega3 scanning electron microscope (SEM) was employed to examine the morphologies of gold-coated samples.

The porosity and pore size distribution of the crushed samples (5–10 mm) was measured by using a mercury intrusion porosimeter (MIP) (Micromeritics Autopore IV) at a maximal pressure of 30,000 psi after vacuum purging. The samples were immersed in acetone for 30 days, followed by oven drying at 60°C for 7 days before subjected to the test.

Results and Discussion

Spectroscopic/Microscopic Characteristics of S/S Treated Sediment

The XRD spectra (Fig. 1) illustrate that quartz, muscovite, illite, and kaolinite were the main minerals in the sediment. After the S/S treatment by combination of OPC and ISSA, ettringite (AFt), and calcite were identified to be the newly formed phases. The usual cement hydration product, calcium silicate hydrates (C-S-H), was not identified mostly due to its amorphous characteristics and relatively low content. But the presence of C-S-H was revealed by the SEM and DTG analysis in the following sections. By comparison, portlandite, calcite, and hydrocalumite were produced in the

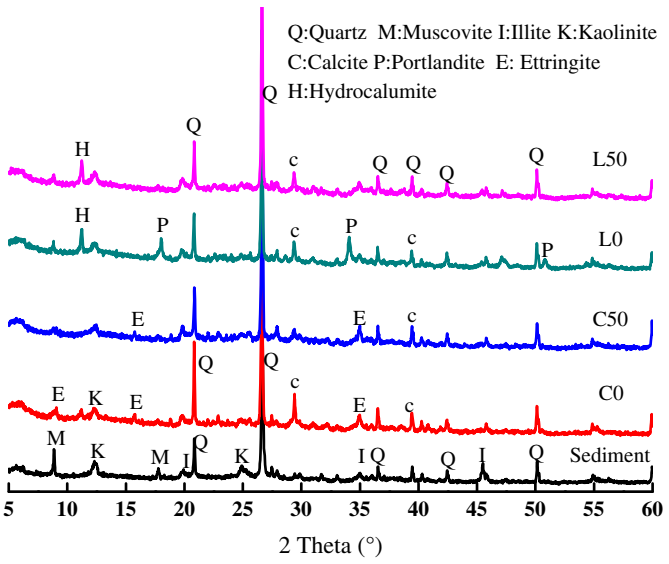

Fig. 1. XRD spectra of 28 day sediment-based samples before and after S/S treatment.

sediment mixtures after S/S treatment by lime and ISSA. Among the OPC treated samples, the inclusion of ISSA decreased the amounts of calcite formed significantly. Note that portlandite was not identified in these mixtures, mostly due to its small content. By contrast, an abundant amount of portlandite from lime hydration was found in the lime–sediment mixtures. However, the sharp peaks of portlandite were depleted after ISSA incorporation, which resulted from the pozzolanic reactions between ISSA and portlandite. Therefore, the ISSA can be an alternative supplementary cementitious material (SCM) for lime-based S/S treated sediments. Note that hydrocalumite was present in the lime–sediment mixtures, mostly because part of soluble Al in the sediments (21.99%) reacted with portlandite produced from lime hydration.

Fig. 2 presents the SEM images of raw materials (sediment and ISSA) and S/S samples C0, C50, L0, and L50 after 28 days of curing. As shown in Fig. 2(a), big plate-like and pillar shape particles were observed in the sediment. Some amorphous particles and fiber-like structures were visible, which were intermixed within the larger particles in the sediment. The SEM image of ISSA shown in Fig. 2(b) indicates the common feature of an irregular morphology with porous structure. The SEM image of sample C0 without ISSA incorporation [Fig. 2(c)] shows the amorphous phases were dominant and covered on the sediment surfaces. The amorphous phases were primarily formed from OPC hydration, such as C-S-H and calcium aluminate hydrates (C-A-H). However, there were many irregular lath/plate-like crystals in sample C50 [Fig. 2(d)], some of which were covered by amorphous hydration products. It can be envisaged that the crystals were primarily from sediment or ISSA. These results indicated that little ISSA-sediment reacted with $Ca(OH)_2$ from OPC hydration and integrated into the formation of hydration products. In addition, incorporation of ISSA might prevent cement hydration to a certain extent due to the existing pollutants in the ISSA (Guo et al. 2017). As shown in Figs. 2(e and f), after the addition of lime, signs of chemical reactions were observed on the surface of sediment and ISSA particles, which might be attributed to the $Ca(OH)_2$ from lime hydration reacting with the sediment and ISSA particles. The needle-like crystals and amorphous phases of hydration products covered most of the exposed surfaces. Hwang et al. (2014) also reported that lime can react with Al and Si to form a Ca-Al-Si gel, which reduced the formation of micropores and consequently improved the compressive strength. Simultaneously, an increase in the aggregates and interaggregate pores was observed in Sample L50 compared with L0, which might be attributed to the bond effects of the newly formed hydration products or the nucleation of ISSA, causing reorganization of the particles and large pores (Li et al. 2015; Chen and Poon 2017).

The DTG test can be used to quantify the composition changes of the sediment mixtures based on the stoichiometric relation with mass loss at a specific temperature. As shown in the TG and DTG curves in Fig. 3, the peaks between 400°C and 550°C possibly correspond to the decomposition of organic matters in the sediment. After the S/S treatment by OPC–lime, these peaks were depleted, primarily due to the destructive effects of the high-alkaline hydration products. Apart from the influences of the sediment, the mass loss between 100°C and 200°C reflected the presence of several hydration products including C-S-H, Aft, and C-A-H (Shen et al. 2017) due to the loss of their chemically bound water. However, the content of each phase could not be calculated by the stoichiometric relation. The peaks between 380°C and 450°C suggested the dehydroxylation of the $Ca(OH)_2$ (CH). The peaks at a higher temperature coincided with the decomposition of carbonates (CC), such as amorphous calcium carbonate (500°C–700°C), metastable vaterite, aragonite (700°C–780°C), and well-crystallized calcite (780°C–900°C) (Wu and Ye 2017).

As shown in Fig. 3(a), for the OPC-based samples, the S/S treatment increased the mass loss between 100°C and 200°C, indicating that the hydration products of cement were present. This coincided with the strength development of the sediment mixtures. With the replacement of OPC by ISSA from 20% to 50%, the content of hydration products was significantly reduced (from 1.812% to 1.576%) but the content of CH was largely increased (from 1.538% to 1.837%). In comparison [shown in Fig. 3(c)], the content of hydration products in the lime-sediment mixtures was lower than the OPC-sediment ones, but the content of hydration products just slightly decreased with the ISSA incorporation (from 1.436% to 1.337%). In addition, the CH content in the lime-sediment mixtures was reduced with ISSA incorporation (from 1.774% to 1.484%). These results verified that the CH in the lime-sediment mixtures reacted with ISSA to generate additional hydration products via pozzolanic reactions. For both types of S/S treatment, the content of CC decreased with ISSA incorporation due to the reduction of CH.

The pores in the stabilized soil can be classified as intra-aggregate pores ($d < 0.01$ μm), small interaggregate pores (0.01 μm $\le d < 0.1$ μm), large interaggregate pores (0.1 μm $\le d < 10$ μm), and air voids ($d > 10$ μm) based on the category of Horpibulsuk et al. (2009). Fig. 4 shows the pore volume distributions of the S/S treated sediment samples. It is found that the total cumulative pore volume (calculating the peak areas) of the OPC-sediment mixtures ranged from 0.40 to 0.45 mL/g, which were larger than that of lime-sediment mixtures (from 0.37 to 0.40 mL/g). This suggested that better bonds were produced in the lime-sediment mixtures than in the OPC-sediment mixtures, which were consistent with the results of SEM that many hydration products were formed and coated on the surface of the lime–ISSA treated sediment. As shown in Fig. 4, the pore size of the OPC-sediment mixtures mainly ranged from 0.02 to 10 μm, namely the interaggregate pores dominated in these samples. The OPC treated samples had a predominant pore diameter of 0.08 μm, but it was shifted to a larger diameter for the samples prepared with ISSA, at around 0.3 μm for Sample C50. Therefore, replacing cement by ISSA increased the porosity of the OPC-sediment samples due to the decrease in the amount of hydration products, which was also verified by the XRD and DTG results. By contrast, two types of pores were present in the lime-sediment mixtures, namely many interaggregate pores with size between 0.03 and 10 μm and small air voids with size between 10 and 100 μm. The predominant pore diameter was around 0.7 μm for these samples and showed a slight decreasing trend with the incorporation of ISSA. Some pores between the sediment particles were filled with the formed cementitious hydration products, which caused the decrease of the amount of small pores. The aggregation of ISSA-sediment particles due to the bonding effect of hydration products tended to increase the air voids between aggregates in samples, and this was also supported by SEM observations.

Engineering Characteristics of S/S Treated Sediment

The stress-strain relationships of the contaminated sediments stabilized/solidified by a combination of OPC–lime and ISSA at 7 and 28 days are shown in Fig. 5. The parameters including UCS, failure strain, and deformation modulus E_{50} can be calculated from the full stress-strain curves. As shown in Figs. 5(a and c) for samples after 7 days of curing, the initial portion (initial strain stage) of the stress-strain curves showed a concave shape, which illustrated that the deformation of samples was increased faster than the stress development. This could be ascribed to the large amount of pores present in the samples (Xue et al. 2014). Afterward, the stress for most samples increased linearly with strain, reflecting an

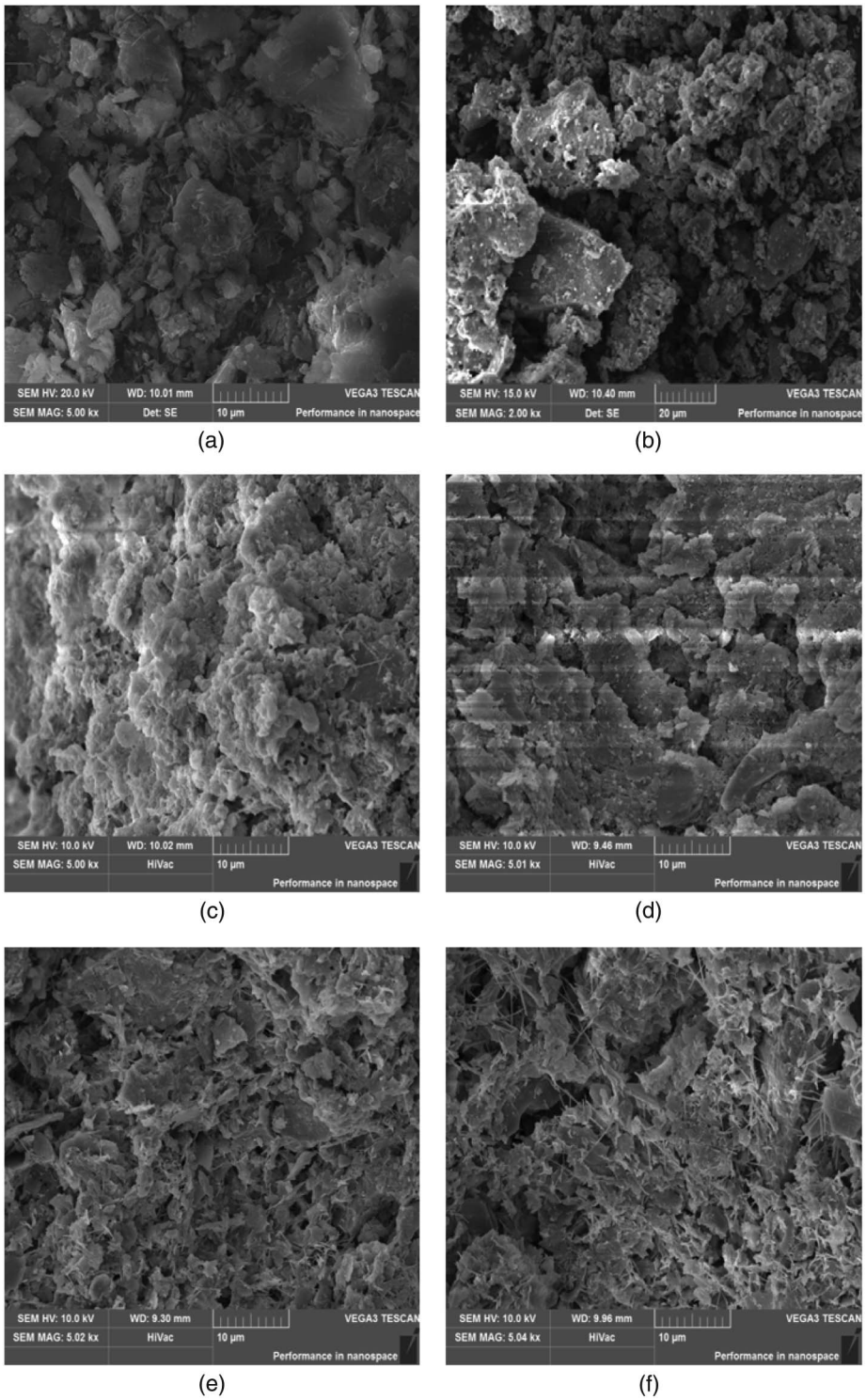

Fig. 2. SEM images of samples: (a) sediment; (b) ISSA; (c) C0; (d) C50; (e) L0; and (f) L50.

elastic strain produced. For the samples solidified by OPC-based treatment, the stress continued to rise until reaching the peak stress. But for the lime–ISSA treated samples, after the linear evolution, the stress increased slowly following a nonlinear trend, suggesting that plastic deformation occurred followed by the peak stress. The peak stress is called as the UCS and the strain at the peak stress is considered as the failure strain. At that moment, some small cracks could be clearly observed on the surface of these samples. After reaching the peak stress, the stress dropped suddenly and gently with an increase in strain for both the OPC-based samples and the lime-based samples. This illustrates that the OPC-based samples were much stiffer and more brittle than the lime-based samples. Finally, the cracks continued to develop and the principal failure appeared.

For the samples after 28 days of curing [Figs. 5(b and d)], the stress increased linearly with strain until the failure strain happened, which was mostly attributed to the high stiffness and compaction of these samples. However, after the peak stress, the lime-treated sediment samples showed an obvious ductility compared with the OPC treated samples.

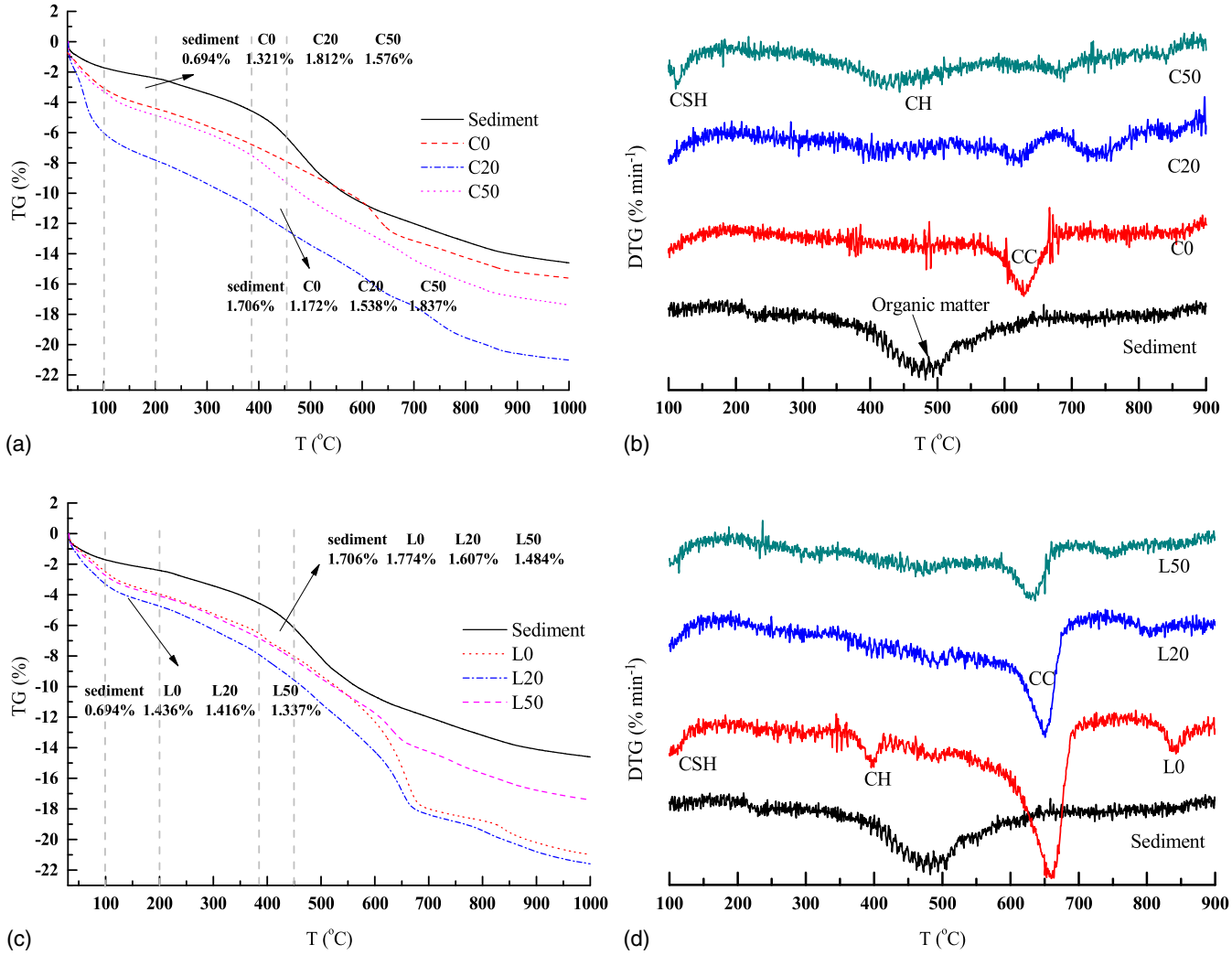

Fig. 3. TG and DTG curves of samples after 28 days of curing: (a) TG curve of OPC treated samples; (b) DTG curve of OPC treated samples; (c) TG curve of lime treated samples; and (d) DTG curve of lime treated samples.

As shown in Fig. 6(a), the UCS of all the sediment mixtures increased with the extension of curing time from 7 to 28 days, but all the values were below the ACI 28 days UCS specification of 1.15 MPa to qualify as a low strength filling material except for samples C0 and C20 after 28 days of curing (ACI 1999). Therefore, from the viewpoint of stress of engineering fills, ISSA–lime treated sediment showed better performance than OPC and OPC–ISSA treated sediment. The UCS of OPC-based sediments were always higher than that of the lime-based sediments as the cement hydration would produce more cementitious binder. With the incorporation of ISSA, the UCS of the OPC-based samples decreased. But an opposite trend was found for the lime-based samples. For instance, the 28 day UCS of the lime-treated sediments increased from 280 to 500 kPa as the replacement level of ISSA was increased from 0% to 50%. The formation of the cementitious binders significantly improved the integrity of the lime–ISSA stabilized sediments and their strength performance. This material had better performance compared with conventional compacted clay under the maximum dry density (Yilmaz 2015). Therefore, considering the low cost of the constituent materials, no need to apply compaction, and low environmental footprint the use of lime–ISSA sediment mixtures as a fill material may be economical and feasible.

For the failure strain shown in Fig. 6(b), it seemed that there was no consistent trend for the OPC treated sediments at different curing times, and the intrinsic explication cannot be demonstrated at present because the complexity of these mixtures and other factors (including strength and porosity) may affect this performance. The failure strain of the lime-treated samples had a decreasing trend with the extension of curing time and ISSA inclusion and this was due to hardening of the mixtures, and the finding was consistent with the results of others (Wang et al. 2013a). Therefore, it could be concluded that an increase in ISSA content enhanced the brittleness of the lime-based sediment samples, while posed an inconspicuous effect on the OPC-based sediment samples. This was primarily related to the pozzolanic reactions between ISSA and lime, which was verified by the spectroscopic/microscopic results. In addition, note that the failure strains of all the S/S treated sediments was between 4% and 6%, and it is necessary to apply a monitoring program in the case of the complex projects construction.

In Fig. 7 note that the UCS of the OPC-based samples decreased after water soaking except for C0, while the UCS of all the lime-based samples increased after water soaking. For the sample C0 after 30 days of further water soaking, $Ca(OH)_2$ could react with the active minerals in the sediments to form additional hydration products, leading to a mild increase of strength of the sediment

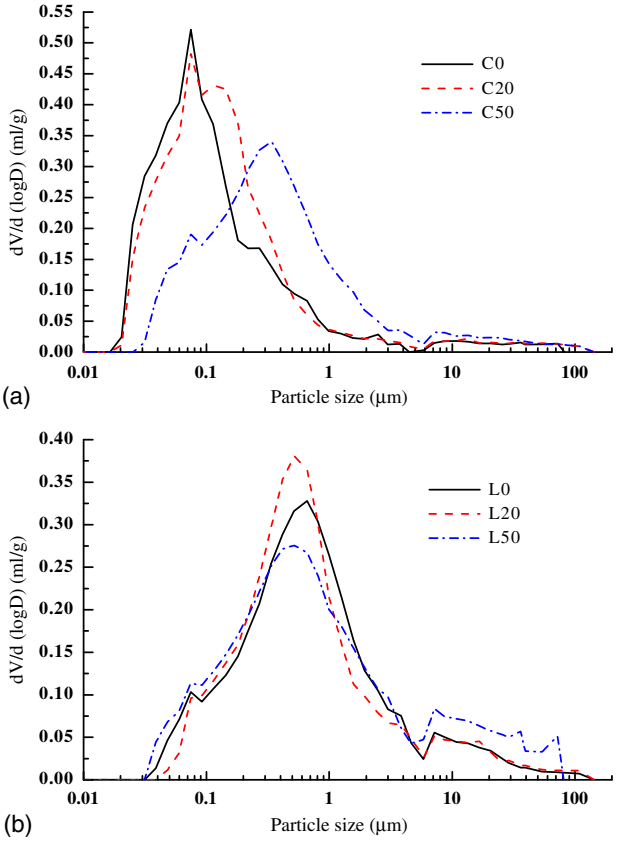

Fig. 4. Pore size distribution of sediment samples treated with (a) OPC; and (b) lime-based binder.

samples. However, $Ca(OH)_2$ in OPC–ISSA binder was too little to activate ISSA and the sediment. Conversely, the hydration products in these sediment samples were partially dissolved under water soaking and hence the strength of the S/S treated sediment samples decreased. For the lime-treated samples, the hydrated lime reacted with the ISSA and sediment minerals in the long-term hydration process and the mechanical properties of the sediment samples were hence improved (Wu et al. 2018). Therefore, the lime–ISSA binder could completely replace OPC–ISSA binder for S/S of contaminated marine sediments as a low strength filling material from the mechanical properties perspective.

The deformation modulus E_{50}, which reflects the deformation resistance capacity of the sediment samples, is an important parameter in the analysis of their settling behavior. Fig. 8 shows the variation of E_{50} with the UCS of the S/S treated sediment samples with different binder mixes and curing times. It can be seen that the variation of E_{50} was quite consistent with the development of UCS, and the linear function could be expressed by $E_{50} = 17.08\text{UCS} + 1{,}331.87$ with R^2 of 0.86. This result was consistent with the previous studies (Lee et al. 2005; Cai et al. 2015), but the mathematical expressions differed from each other due to the differences in the matrixes and the binders used. In addition, this result also confirmed that the incorporation of ISSA had a strengthening effect on the lime-treated sediments, but had a weakening effect on the OPC-treated sediments.

The shear strength of a material is a function of intergranular frictional resistance and cohesion, which determines the ability to support the imposed stresses on the material. According to the test results shown in Table 2, the cohesion values of the S/S sediments ranged from 53 to 186 kPa and the angles of shearing resistance ranged from 30° to 39°. The value for angle of shearing resistance is between 40° and 55° for the consolidated-drained medium size gravely soil while the minimum value is between 20° and 22° for the unconsolidated-undrained silty sand soil (Bowles 1996). Accordingly, the angle of shearing resistance values of the S/S treated sediment mixtures fell between the range of the medium size gravely soil and the silty sand soil. Generally, it can be noted that the OPC-based samples showed a higher shearing resistance performance than the lime-based samples, no matter how the curing time and ISSA incorporation amount changed.

As shown in Table 2, adding ISSA into the mixture of the sediments and OPC caused a decrease in the cohesion but had a negligible effect on the internal friction angle. The decrease in hydration products due to the ISSA incorporation contributed to the reduction in the bond strength. However, the decrease in bonding due to fewer hydration products could be compensated by the increased friction provided by the ISSA incorporation. This could be explained by the fact that the irregular ISSA particles provide better friction between the particles. As a comparison, adding ISSA into the mixture of sediments and lime caused increases in both the cohesion and internal friction angle parameters because of the additional formation of the hydration products and the friction provided by the irregular ISSA particles. The test results also indicated that the sediment-based S/S mixtures have the superior shear strength properties compared to the general compacted soils (Li et al. 2013), so it has been proven that they are suitable for use in backfill applications.

Fig. 9 shows the water permeability of the OPC–lime stabilized sediments. The permeability of all S/S treated samples decreased with curing time due to the increase in cementitious hydrations and associated bonding strength. Generally, the permeability of the OPC treated sediments was lower than that of the lime treated sediments, and the permeability values of all the samples ranged from 5.0×10^{-8} to 4.5×10^{-7} m/s, which was consistent with that of previous study on the lime and cement stabilized natural clayey soils (Onitsuka et al. 2001). The differences in the permeability between OPC and lime treated sediments might be dependent on the volume of air pores (>10 μm), and this was also found in the previous studies and verified by the MIP results of this study (Du et al. 2017). The coefficient of permeability of the OPC-based samples increased with the increasing ISSA content. The pore spaces of the OPC-based samples with ISSA were increased because of the reductions of the formed cementing hydration products as shown before [Fig. 2(a)], which agreed well with the DTG [Fig. 3(a)] and MIP [Fig. 4(a)] results. However, the permeability decreased with the increase in ISSA content in the lime-based samples. Therefore, the sediment-lime mixtures with more ISSA showed better durability because they were less permeable compared with the OPC-sediment mixtures. The permeability is directly related to the porosity in the samples. As shown in Fig. 4(b), the ISSA incorporation decreased the predominant pore diameters in the lime-treated samples due to the formation of more cementitious hydration products. However, although the air voids increased slightly with the ISSA incorporation, the long-term hydration between $Ca(OH)_2$ and ISSA with water infiltration rearranged the pore structures, and caused the decrease of permeability. This is also consistent with the results found in Fig. 7 that the long-term soaking of the lime-sediment samples could increase the bonding and strength.

Environmental Risk of S/S Treated Sediment

The environmental risk of the S/S sediment materials is a big concern because a certain amount of metal(loid)s are presented in the sediments and ISSA (Li et al. 2017d). As shown in Fig. 10

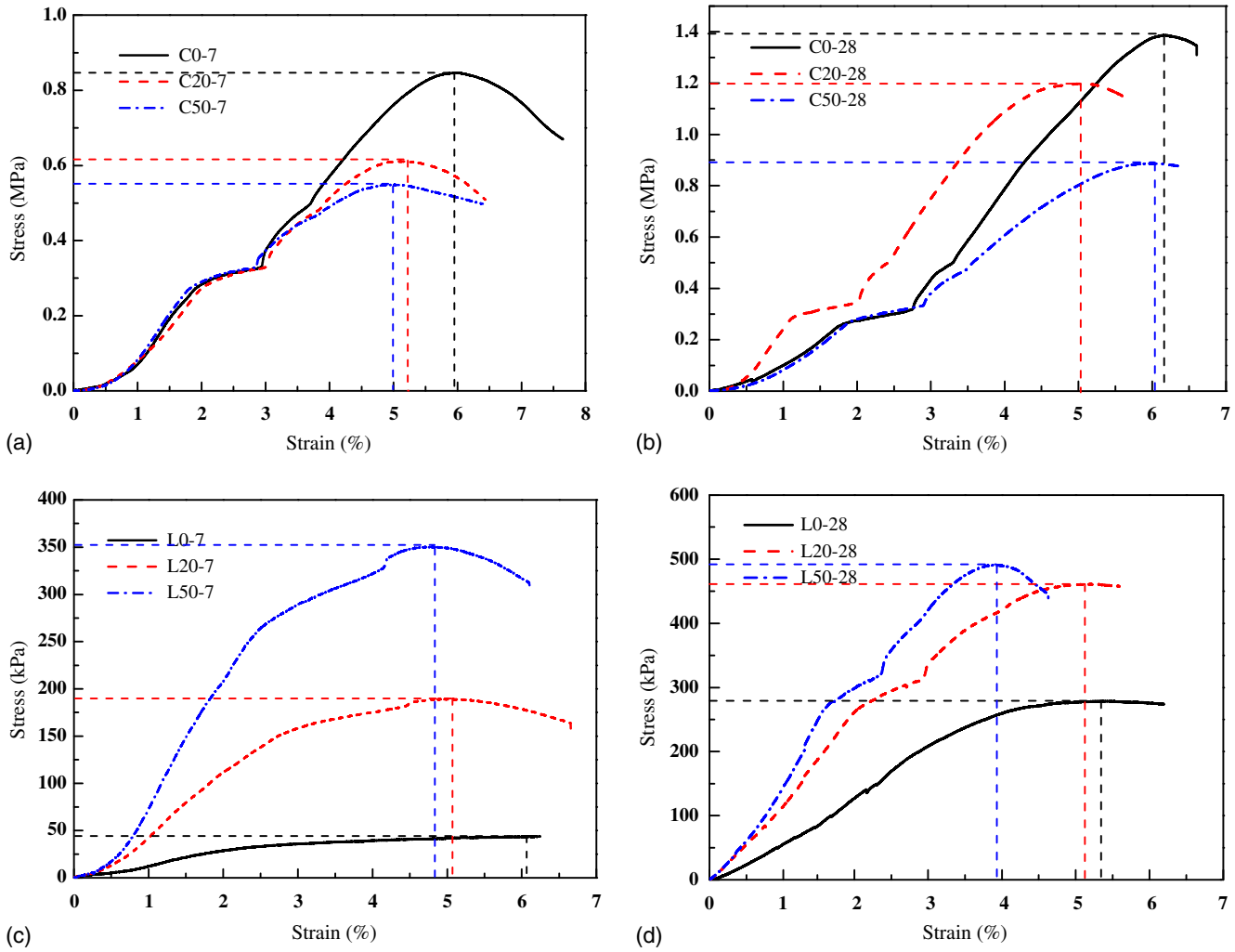

Fig. 5. Strain-stress curves of samples (dotted line in the figures denotes UCS and its corresponding failure strain): (a) OPC-based treatment after curing for 7 days; (b) OPC-based treatment after curing for 28 days; (c) lime-based treatment after curing for 7 days; and (d) lime-based treatment after curing for 28 days.

(only detectable and concerned metals are given), the leachability of Cu (0.12 mg L^{-1}), Zn (1.33 mg L^{-1}), Pb (0.14 mg L^{-1}), and As (0.05 mg L^{-1}) from the raw sediments did not exceed the universal treatment standard in Hong Kong (HK EPD 2011). Thus, the contaminated sediments could be acceptable for the direct reuse, but the environmental risk still exists when they are exposed to the extreme field conditions (e.g., varying pH, runoff, and redox conditions). After the S/S treatment by ISSA-based binders, the potential toxic metals from the contaminated sediments were stabilized, especially by the lime–ISSA binders. This confirmed that the cementitious hydration products could effectively stabilize the contaminants by physical encapsulation and/or chemical fixation (Li et al. 2017c). Note that the S/S treatment had little effect on the leachability of As, mostly because of its high alkali-soluble characteristics (Li et al. 2017a). For the OPC–ISSA-based treatment, the ISSA incorporation increased the leachability of Zn, Cu, and Pb, which was opposite for the lime–ISSA-based treatment, except for Zn. These inconsistent behaviors were associated with the changes in pH and metal species (Li et al. 2017b).

According to the TCLP test results, the ISSA-sediment products were environmentally acceptable. This can be also verified by the semidynamic leaching test results on the monolithic samples shown in Figs. 11, S2, and S3. Negligible toxic metals were leached from the S/S samples, and only very small amounts of Cu, Pb, and As could be detected. In the long-term leaching, the concentrations of leached Cu, Pb, and As ranged from 1 to 22 μg/L, 1 to 9 μg/L, and 13 to 28 μg/L, respectively. Thus, the S/S treated contaminated sediments could be used for construction applications with minimal leaching concerns. In addition, the leaching of these metals were mainly diffusion controlled (Li et al. 2017c), and the effective diffusion coefficient of Cu, Pb, and As were in the range of 1.49×10^{-11} m^2/s to 5.63×10^{-11} m^2/s, 1.09×10^{-12} m^2/s to 7.83×10^{-12} m^2/s, and 8.49×10^{-9} m^2/s to 1.31×10^{-8} m^2/s, respectively, indicating the low mobility and the difficulties of releasing these metals (Xue et al. 2017).

Overall, combining the engineering and environmental (leaching) characteristics of S/S sediments, the lime–ISSA binder can be successfully applied for S/S treatment of contaminated marine sediments with high moisture content as a low-strength filling material. A general mix design based on blending 50% of lime with ISSA is recommended as the most effective binder to achieve a relatively high strength and low leachability of metal(loid)s. However, the optimal amount of lime–ISSA binder should be determined according to the properties of the specific contaminated sediment to be

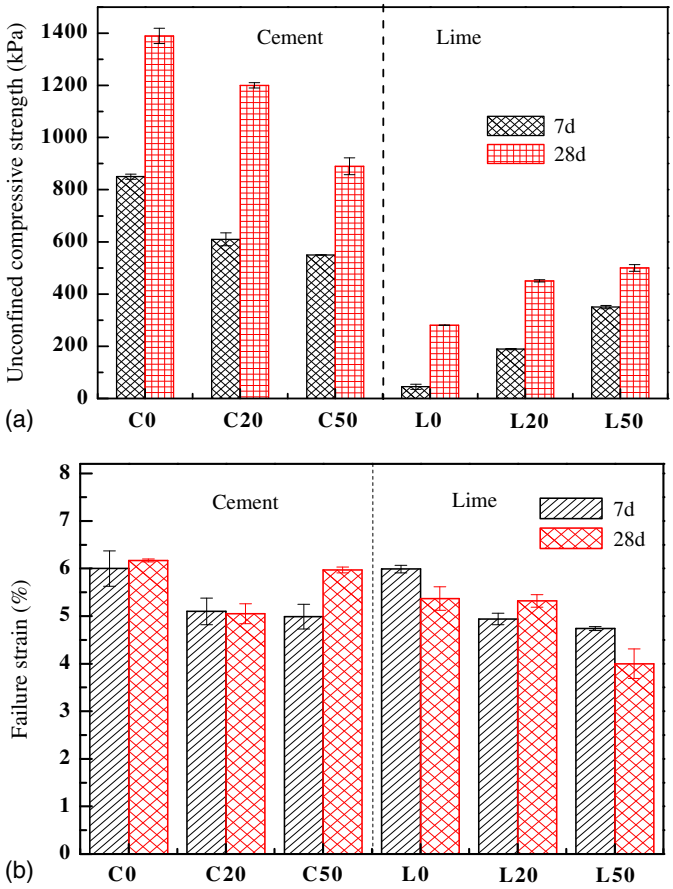

Fig. 6. (a) UCS and (b) failure strain of S/S treated sediment samples.

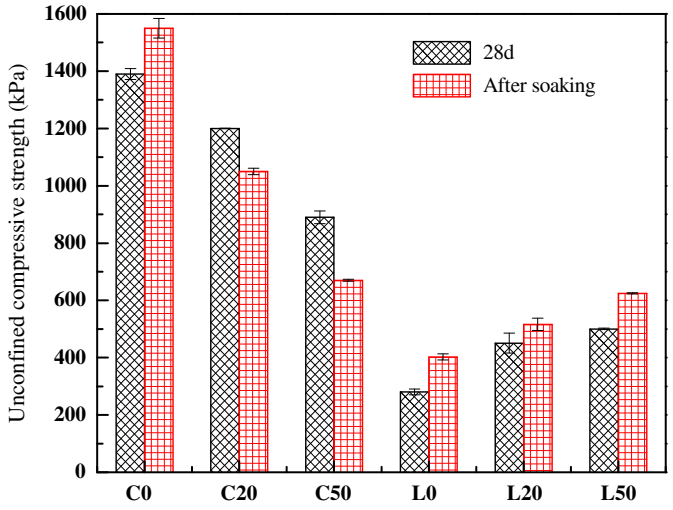

Fig. 7. UCS of S/S treated sediment samples before and after water soaking.

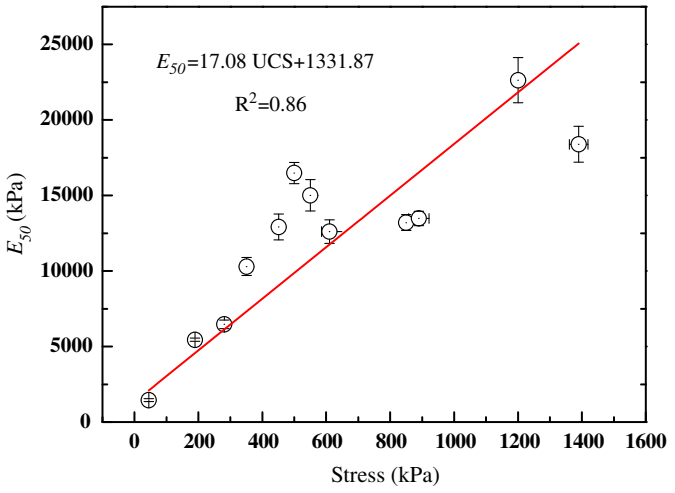

Fig. 8. Relationship between deformation modulus and UCS.

Table 2. Direct shear test results at 3 days

Parameters	Mixtures					
	C0	C20	C50	L0	L20	L50
Cohesion intercept (kPa)	186	138	125	53	62	106
Angle of shearing resistance (degrees)	39	37	38	30	34	35

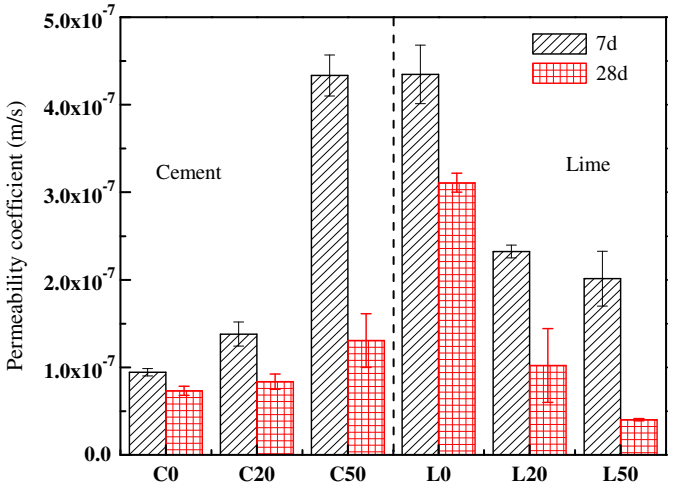

Fig. 9. Permeability coefficient of S/S treated sediment samples.

Conclusions

This study evaluated the feasibility of developing a novel S/S process by incorporating ISSA into OPC–lime as a binder to stabilize contaminated sediments. The following conclusions can be drawn.

- It was found that using lime–ISSA as a binder has several advantages over OPC–ISSA binder owing to its lower cost, good ability to recycle wastes, lower environmental footprints, and better strength gains.
- The addition of ISSA improved the compressive and shear strengths, deformation resistance, and durability of the lime-treated sediments. This can be attributed to the reactions

treated, including moisture content, organic matter content, particle size distribution, and chemical compositions. Indeed, each project site has unique sediment conditions and functional requirements, thus detailed on-site pilot-scale trials should be carried out to demonstrate the suitability of the binder material, methods, and equipment used for processing, and also the methods of backfilling of the treated sediments to meet the treatment targets.

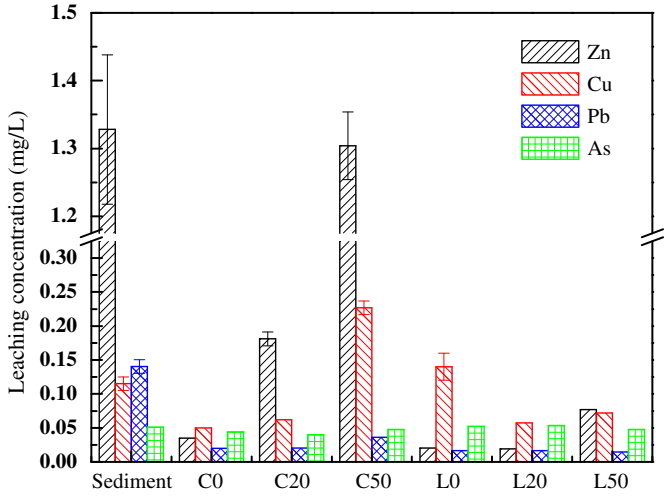

Fig. 10. TCLP leachability of metal(loid)s from S/S treated samples.

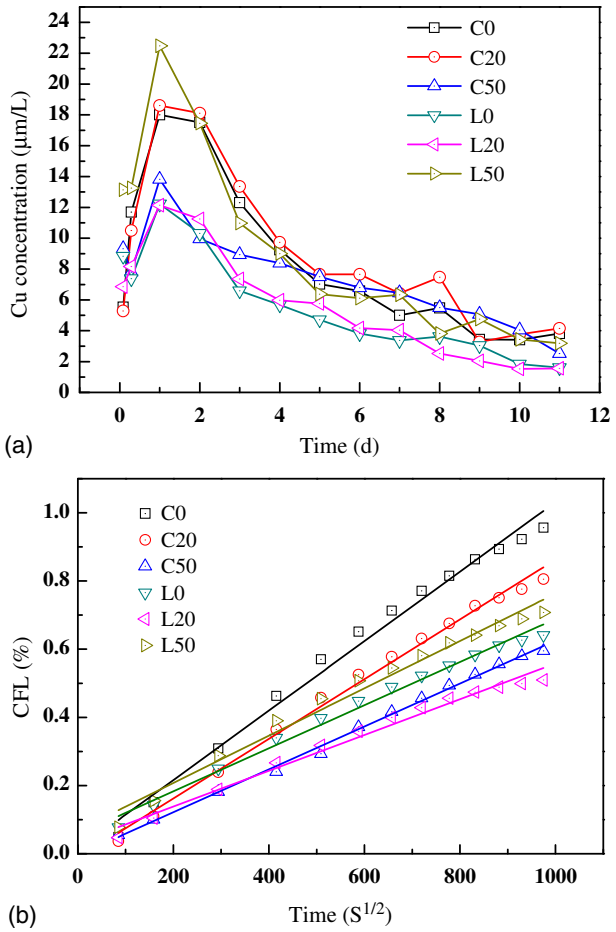

Fig. 11. Leaching concentration and cumulative fraction leached of Cu: (a) Cu concentration; and (b) cumulative fraction leached (CFL).

between ISSA and lime and the associated formation of cementitious hydration products.

- In addition, based on the TCLP and dynamic leaching test results, it can be concluded that the leachate from the stabilized sediments was not harmful to the environment. Therefore, this study presents an economically sustainable, environmentally clean, and technologically feasible method for transforming ISSA and contaminated dredged marine sediment wastes into a very useful fill material.
- However, further studies are required to explore the following areas: (1) characterization of ISSA activated by lime using conventional and advanced spectroscopic techniques, and (2) development of technology and economically effective methods for full-scale production of the ISSA–lime binder and its application in S/S treatment of dredged marine sediment.

Data Availability Statement

All data, models, and code generated or used during the study appear in the submitted article.

Acknowledgments

The authors would like to thank the financial support of the National Natural Science Foundation of China (41602315 and 51625903), the National Natural Science Foundation of China/Hong Kong Research Grants Council Joint Research Scheme under Grant Nos. N_PolyU511/18, 51861165104, and the Open Research Fund of State Key Laboratory of Geomechanics and Geotechnical Engineering, Institute of Rock and Soil Mechanics, Chinese Academy of Sciences (No. Z015003).

Supplemental Data

Figs. S1–S3 are available online in the ASCE Library (www.ascelibrary.org).

References

Achour, R., N. E. Abriak, R. Zentar, P. Rivard, and P. Gregoire. 2014. "Valorization of unauthorized sea disposal dredged sediments as a road foundation material." *Environ. Technol.* 35 (16): 1997–2007. https://doi.org/10.1080/09593330.2014.889758.

ACI (American Concrete Institute). 1999. *Controlled low strength materials*. ACI 229R. Farmington Hills, MI: ACI.

ASTM. 2007. *Standard test method for flow of hydraulic cement mortar*. ASTM C1437. West Conshohocken, PA: ASTM.

ASTM. 2008. *Standard test method for accelerated leach test for diffusive releases from solidified waste and a computer program to model diffusive. Fractional leaching from cylindrical waste forms*. ASTM C1308. West Conshohocken, PA: ASTM.

Bowles, L. E. 1996. *Foundation analysis and design*. New York: McGraw-Hill.

BSI (British Standards Institution). 1990a. *Methods of test for soils for civil engineering purposes: Compressibility, permeability and durability tests*. BSI BS 1377-5. London: BSI.

BSI (British Standards Institution). 1990b. *Methods of test for soils for civil engineering purposes—Part 7: Shear strength tests (total stress)*. BSI BS 1377-7. London: BSI.

BSI (British Standards Institution). 2002. *Testing hardened concrete–Part 3: Compressive strength of test specimens*. EN 12390-3. London: BSI.

Cai, G. H., S. Y. Liu, Y. J. Du, D. W. Zhang, and X. Zheng. 2015. "Strength and deformation characteristics of carbonated reactive magnesia treated silt soil." *J. Central South Univ.* 22 (5): 1859–1868. https://doi.org/10.1007/s11771-015-2705-5.

Chatain, V., M. Benzaazoua, M. L. Cazalet, H. Bouzahzah, C. Delolme, M. Gautier, D. Blanc, and C. De Brauer. 2013. "Mineralogical study and leaching behavior of a stabilized harbor sediment with hydraulic binder." *Environ. Sci. Pollut. Res.* 20 (1): 51–59. https://doi.org/10.1007/s11356-012-1141-4.

Chen, L., and D. F. Lin. 2009. "Stabilization treatment of soft subgrade soil by sewage sludge ash and cement." *J. Hazard. Mater.* 162 (1): 321–327. https://doi.org/10.1016/j.jhazmat.2008.05.060.

Chen, Z., J. S. Li, and C. S. Poon. 2018a. "Combined use of sewage sludge ash and recycled glass cullet for the production of concrete blocks." *J. Cleaner Prod.* 171 (Jan): 1447–1459. https://doi.org/10.1016/j.jclepro.2017.10.140.

Chen, Z., J. S. Li, B. J. Zhan, U. Sharma, and C. S. Poon. 2018b. "Compressive strength and microstructural properties of dry-mixed geopolymer pastes synthesized from GGBS and sewage sludge ash." *Constr. Build. Mater.* 182 (Sep): 597–607. https://doi.org/10.1016/j.conbuildmat.2018.06.159.

Chen, Z., and C. S. Poon. 2017. "Comparative studies on the effects of sewage sludge ash and fly ash on cement hydration and properties of cement mortars." *Constr. Build. Mater.* 154 (Nov): 791–803. https://doi.org/10.1016/j.conbuildmat.2017.08.003.

Couvidat, J., V. Chatain, H. Bouzahzah, and M. Benzaazoua. 2018. "Characterization of how contaminants arise in a dredged marine sediment and analysis of the effect of natural weathering." *Sci. Total Environ.* 624 (May): 323–332. https://doi.org/10.1016/j.scitotenv.2017.12.130.

Cyr, M., M. Coutand, and P. Clastres. 2007. "Technological and environmental behavior of sewage sludge ash (SSA) in cement-based materials." *Cem. Concr. Res.* 37 (8): 1278–1289. https://doi.org/10.1016/j.cemconres.2007.04.003.

Dang, T. A., S. Kamali-Bernard, and W. A. Prince. 2013. "Design of new blended cement based on marine dredged sediment." *Constr. Build. Mater.* 41 (Apr): 602–611. https://doi.org/10.1016/j.conbuildmat.2012.11.088.

Du, Y. J., B. W. Yu, K. Liu, N. J. Jiang, and M. D. Liu. 2017. "Physical, hydraulic, and mechanical properties of clayey soil stabilized by lightweight alkali-activated slag geopolymer." *J. Mater. Civ. Eng.* 29 (2): 04016217. https://doi.org/10.1061/(ASCE)MT.1943-5533.0001743.

Falciglia, P. P., C. Ingrao, G. De Guidi, A. Catalfo, G. Finocchiaro, M. Farina, M. Liali, G. Lorenzano, G. Valastro, and F. G. Vagliasindi. 2018. "Environmental life cycle assessment of marine sediment decontamination by citric acid enhanced-microwave heating." *Sci. Total Environ.* 619 (Apr): 72–82. https://doi.org/10.1016/j.scitotenv.2017.11.085.

Guo, B., B. Liu, J. Yang, and S. Zhang. 2017. "The mechanisms of heavy metal immobilization by cementitious material treatments and thermal treatments: A review." *J. Environ. Manage.* 193 (May): 410–422. https://doi.org/10.1016/j.jenvman.2017.02.026.

HK EPD (Hong Kong Environmental Protection Department). 2011. *Practice guide for investigation and remediation of contaminated land*. Hong Kong: HK EPD.

HK ETWB (Hong Kong: Environment, Transport, and Works Bureau). 2002. *Management of dredged/excavated sediment*. Technical Circular (Works) No. 34/2002. ETWB(W) 209/32/96. Hong Kong: Environment, Transport, and Works Bureau.

Horpibulsuk, S., R. Rachan, and Y. Raksachon. 2009. "Role of fly ash on strength and microstructure development in blended cement stabilized silty clay." *Soils Found.* 49 (1): 85–98. https://doi.org/10.3208/sandf.49.85.

Hwang, K. Y., J. Y. Seo, H. Q. Phan, J. Y. Ahn, and I. Hwang. 2014. "MgO-based binder for treating contaminated sediments: Characteristics of metal stabilization and mineral carbonation." *CLEAN–Soil, Air, Water* 42 (3): 355–363. https://doi.org/10.1002/clen.201200663.

Lee, F. H., Y. Lee, S. H. Chew, and K. Y. Yong. 2005. "Strength and modulus of marine clay-cement mixes." *J. Geotech. Geoenviron. Eng.* 131 (2): 178–186. https://doi.org/10.1061/(ASCE)1090-0241(2005)131:2(178).

Li, J. S., J. Beiyuan, D. C. Tsang, L. Wang, C. S. Poon, X. D. Li, and S. Fendorf. 2017a. "Arsenic-containing soil from geogenic source in Hong Kong: Leaching characteristics and stabilization/solidification." *Chemosphere* 182 (Sep): 31–39. https://doi.org/10.1016/j.chemosphere.2017.05.019.

Li, J. S., and C. S. Poon. 2017. "Innovative solidification/stabilization of lead contaminated soil using incineration sewage sludge ash." *Chemosphere* 173 (Apr): 143–152. https://doi.org/10.1016/j.chemosphere.2017.01.065.

Li, J. S., D. C. Tsang, Q. M. Wang, L. Fang, Q. Xue, and C. S. Poon. 2017b. "Fate of metals before and after chemical extraction of incinerated sewage sludge ash." *Chemosphere* 186 (Nov): 350–359. https://doi.org/10.1016/j.chemosphere.2017.08.012.

Li, J. S., L. Wang, D. C. Tsang, J. Beiyuan, and C. S. Poon. 2017c. "Dynamic leaching behavior of geogenic as in soils after cement-based stabilization/solidification." *Environ. Sci. Pollut. Res.* 24 (36): 27822–27832. https://doi.org/10.1007/s11356-017-0266-x.

Li, J. S., Q. Xue, L. Fang, and C. S. Poon. 2017d. "Characteristics and metal leachability of incinerated sewage sludge ash and air pollution control residues from Hong Kong evaluated by different methods." *Waste Manage.* 64 (Jun): 161–170. https://doi.org/10.1016/j.wasman.2017.03.033.

Li, J. S., Q. Xue, P. Wang, and Z. Z. Li. 2015. "Effect of lead (II) on the mechanical behavior and microstructure development of a Chinese clay." *Appl. Clay Sci.* 105 (Mar): 192–199. https://doi.org/10.1016/j.clay.2014.12.030.

Li, J. S., Q. Xue, P. Wang, and L. Liu. 2013. "Influence of leachate pollution on mechanical properties of compacted clay: A case study on behaviors and mechanisms." *Eng. Geol.* 167 (Dec): 128–133. https://doi.org/10.1016/j.enggeo.2013.10.013.

Libralato, G., D. Minetto, G. Lofrano, M. Guida, M. Carotenuto, F. Aliberti, B. Conte, and M. Notarnicola. 2018. "Toxicity assessment within the application of in situ contaminated sediment remediation technologies: A review." *Sci. Total Environ.* 621 (Apr): 85–94. https://doi.org/10.1016/j.scitotenv.2017.11.229.

Lofrano, G., G. Libralato, D. Minetto, S. De Gisi, F. Todaro, B. Conte, D. Calabrò, L. Quatraro, and M. Notarnicola. 2017. "In situ remediation of contaminated marine sediment: An overview." *Environ. Sci. Pollut. Res.* 24 (6): 5189–5206. https://doi.org/10.1007/s11356-016-8281-x.

Onitsuka, K., C. Modmoltin, and M. Kouno. 2001. "Investigation on microstructure and strength of lime and cement stabilized Ariake clay." *Rep. Faculty Sci. Eng. Saga Univ.* 30 (1): 49–63.

Saussaye, L., H. Hamdoun, L. Leleyter, E. van Veen, J. Coggan, G. Rollinson, W. Maherzi, M. Boutouil, and F. Baraud. 2016. "Trace element mobility in a polluted marine sediment after stabilisation with hydraulic binders." *Mar. Pollut. Bull.* 110 (1): 401–408. https://doi.org/10.1016/j.marpolbul.2016.06.035.

Shen, P., L. Lu, Y. He, F. Wang, and S. Hu. 2017. "Hydration of quaternary phase-gypsum system." *Constr. Build. Mater.* 152 (Oct): 145–153. https://doi.org/10.1016/j.conbuildmat.2017.06.179.

Shim, J. H., J. Y. Jeong, J. Y. Park, J. S. Ryu, and J. Y. Park. 2016. "Characterization of alkali-activated slag paste containing dredged marine sediment." *Desalin. Water Treat.* 57 (51): 24688–24696. https://doi.org/10.1080/19443994.2016.1157993.

Tang, I. Y., D. Y. Yan, I. M. Lo, and T. Liu. 2015. "Pulverized fuel ash solidification/stabilization of waste: Comparison between beneficial reuse of contaminated marine mud and sediment." *J. Environ. Eng. Landscape Manage.* 23 (3): 202–210. https://doi.org/10.3846/16486897.2015.1021699.

US EPA. 1992. *Method 1311: Toxicity characteristic leaching procedure*. Washington, DC: US EPA.

Wang, D., N. E. Abriak, and R. Zentar. 2013a. "Strength and deformation properties of Dunkirk marine sediments solidified with cement, lime and fly ash." *Eng. Geol.* 166 (Nov): 90–99. https://doi.org/10.1016/j.enggeo.2013.09.007.

Wang, D., N. E. Abriak, R. Zentar, and W. Chen. 2013b. "Effect of lime treatment on geotechnical properties of Dunkirk sediments in France." *Road Mater. Pavement Des.* 14 (3): 485–503. https://doi.org/10.1080/14680629.2012.755935.

Wang, D., R. Zentar, N. E. Abriak, and S. Di. 2018a. "Long-term mechanical performance of marine sediments solidified with cement, lime, and fly ash." *Mar. Georesour. Geotechnol.* 36 (1): 123–130. https://doi.org/10.1080/1064119X.2017.1320600.

Wang, L., L. Chen, D. C. W. Tsang, J. S. Li, K. Baek, D. Hou, S. Ding, and C. S. Poon. 2018b. "Recycling dredged sediment into fill materials, partition blocks, and paving blocks: Technical and economic assessment." *J. Cleaner Prod.* 199 (Oct): 69–76. https://doi.org/10.1016/j.jclepro.2018.07.165.

Wang, L., L. Chen, D. C. W. Tsang, J. S. Li, T. L. Yeung, S. Ding, and C. S. Poon. 2018c. "Green remediation of contaminated sediment by stabilization/solidification with industrial by-products and CO_2 utilization." *Sci. Total Environ.* 631 (Aug): 1321–1327. https://doi.org/10.1016/j.scitotenv.2018.03.103.

Wang, L., K. M. Iris, D. C. W. Tsang, S. Li, J. S. Li, C. S. Poon, Y. S. Wang, and J. G. Dai. 2017a. "Transforming wood waste into water-resistant magnesia-phosphate cement particleboard modified by alumina and red mud." *J. Cleaner Prod.* 168 (Dec): 452–462. https://doi.org/10.1016/j.jclepro.2017.09.038.

Wang, L., D. C. W. Tsang, and C. S. Poon. 2015. "Green remediation and recycling of contaminated sediment by waste-incorporated stabilization/solidification." *Chemosphere* 122 (Mar): 257–264. https://doi.org/10.1016/j.chemosphere.2014.11.071.

Wang, L., T. L. Yeung, A. Y. Lau, D. C. W. Tsang, and C. S. Poon. 2017b. "Recycling contaminated sediment into eco-friendly paving blocks by a combination of binary cement and carbon dioxide curing." *J. Cleaner Prod.* 164 (Oct): 1279–1288. https://doi.org/10.1016/j.jclepro.2017.07.070.

Wu, B., and G. Ye. 2017. "Development of porosity of cement paste blended with supplementary cementitious materials after carbonation." *Constr. Build. Mater.* 145 (Aug): 52–61. https://doi.org/10.1016/j.conbuildmat.2017.03.176.

Wu, M., Y. Zhang, G. Liu, Z. Wu, Y. Yang, and W. Sun. 2018. "Experimental study on the performance of lime-based low carbon cementitious materials." *Constr. Build. Mater.* 168 (Apr): 780–793. https://doi.org/10.1016/j.conbuildmat.2018.02.156.

Xue, Q., J. S. Li, and L. Liu. 2014. "Effect of compaction degree on solidification characteristics of Pb-contaminated soil treated by cement." *CLEAN–Soil, Air, Water* 42 (8): 1126–1132. https://doi.org/10.1002/clen.201300345.

Xue, Q., P. Wang, J. S. Li, T. T. Zhang, and S. Y. Wang. 2017. "Investigation of the leaching behavior of lead in stabilized/solidified waste using a two-year semi-dynamic leaching test." *Chemosphere* 166 (Jan): 1–7. https://doi.org/10.1016/j.chemosphere.2016.09.059.

Yan, D. Y., I. Y. Tang, and I. M. Lo. 2014. "Development of controlled low-strength material derived from beneficial reuse of bottom ash and sediment for green construction." *Constr. Build. Mater.* 64 (Aug): 201–207. https://doi.org/10.1016/j.conbuildmat.2014.04.087.

Yilmaz, Y. 2015. "Compaction and strength characteristics of fly ash and fiber amended clayey soil." *Eng. Geol.* 188 (Apr): 168–177. https://doi.org/10.1016/j.enggeo.2015.01.018.

Zentar, R., D. Wang, N. E. Abriak, M. Benzerzour, and W. Chen. 2012. "Utilization of siliceous-aluminous fly ash and cement for solidification of marine sediments." *Constr. Build. Mater.* 35 (Oct): 856–863. https://doi.org/10.1016/j.conbuildmat.2012.04.024.